ISSN 2359-6562 (ONLINE) 2359-6562 (CD-ROM)

CONCENTRATED SOLAR THERMAL DIRECT STEAM GENERATION FOR SUGAR CANE SPARE

RENAN DE SOUZA CARVALHO[1], JOSÉ ROBERTO SIMÕES MOREIRA[2], CELSO EDUARDO LINS DE OLIVEIRA[3]

[1]Instituto de Energia e Ambiente (IEE), Universidade de São Paulo (USP). Av. Prof. Luciano Gualberto, 1289, Butantã, 05508-010, São Paulo/SP, Brasil. E-mail: renan2.scarvalho@gmail.com
[2]Departamento de Engenharia Mecânica, Escola Politécnica, Universidade de São Paulo (USP). Av. Prof. Mello Moraes, 2231, Butantã, 05508-900, São Paulo, São Paulo, Brasil. E-mail: jrsimoes@usp.br
[3]Departamento de Engenharia de Biossistemas, Faculdade de Zootecnia e Engenharia de Alimentos (FZEA), Universidade de São Paulo (USP). Av. Duque de Caxias Norte, 225, Campus Pirassununga, 13635-900, Pirassununga, São Paulo, Brasil. E-mail: celsooli@usp.br

ABSTRACT: Brazil has a high dependence over oil for energy and heat, and hydropower plants for electricity generation. However, sugar cane bagasse has been increasing its participation over the Brazilian matrix. Nevertheless, its harvest is seasonal. Thus, spare bagasse to be used in complementary periods is a crucial point for a higher flexibility in electricity generation. In this scenario, a central receiver plant was designs to directly generate steam. A solar field layout was obtained through *SolarPILOT* to partially supply the heat demand of a sugar cane bagasse plant located in Pirassununga, SP, Brazil. Three days within the harvest were arbitrarily chosen for a numerical simulation to calculate the spare of bagasse (April 16th, July 16th, and October 16th, 2017), as well as the entire harvest. In the best-case scenario, October 16th, a total spare of 11.1 tons of bagasse was achieved, which represented 0.57% of the total amount of bagasse in a day, whereas in November the spare resulted in 0.50% of the total demand.

Keywords: Concentrated solar thermal, sugar cane bagasse, direct steam generation, SolarPILOT, numerical simulation.

GERAÇÃO DIRETA DE VAPOR COM CONCENTRAÇÃO SOLAR TÉRMICA PARA REDUÇÃO DO CONSUMO DE BAGAÇO DE CANA-DE-AÇÚCAR

RESUMO: O Brasil possui atualmente uma grande dependência de petróleo para geração de energia e calor, bem com usinas hidroelétricas para geração de eletricidade. Entretanto, o bagaço de cana-de-açúcar vem apresentando uma crescente participação na matriz nacional. Todavia, sua colheita é sazonal. Destarte, poupar bagaço para que ele seja utilizado em períodos complementares é um ponto crucial para uma maior flexibilização na geração de eletricidade por parte das usinas. Neste cenário, uma usina solar com receptor central foi dimensionada para geração direta de vapor. Seu *layout* foi obtido através do *software SolarPILOT*, visando suprir parcialmente a demanda de calor de uma usina de cana-de-açúcar localizada em Pirassununga, São Paulo, Brasil. Foram escolhidos três dias arbitrariamente para a simulação do bagaço poupado, sendo eles 16 de abril, 16 de julho, e 16 de outubro de 2017, como também todo o período colheita. Um total de 11,1 toneladas de bagaço poupado foi encontrado o melhor cenário, 16 de outubro, o que representa 0,57% da demanda diária de bagaço da usina, enquanto na análise mensal, novembro apresentou-se com o melhor resultado, atingindo 0,50% da demanda mensal. A biomassa total poupada estenderia a geração por somente mais um dia.

Palavras-chave: concentração solar térmica, bagaço de cana-de-açúcar, geração direta de vapor, SolarPILOT, simulação numérica.

Recebido em 28/09/2020 e aprovado para publicação em 10/05/2021
DOI: http://dx.doi.org/10.17224/EnergAgric.2021v36n1p72-85

1 INTRODUCTION

Brazil, like the rest of the world, still relies over nonrenewable sources to supply its domestic energy demand. According to the Energy Balance Report of 2020 from the Energetic Research Company ("*Empresa de Pesquisa Energética*" – EPE) with data from 2019, oil, and its byproducts still represented most of the domestic energy offer (EMPRESA DE PESQUISA ENERGÉTICA, 2020). However, a renewable source has been carrying a significant presence over the past years regarding the domestic energy offer: sugar cane bagasse. As an example, in 2017, the bagasse itself had a share of 12% of this domestic energy offer, whereas the ethanol, produced mainly by bagasse represented 6%, and the electricity, where biomass represented 8%, the sugar cane has most of 83% (EMPRESA DE PESQUISA ENERGÉTICA, 2018; RAMOS; NACHILUK, 2017).

In 2019, sugar cane and its byproducts represented 16.2% of the total primary energy production, and 39.5% of the renewable share (41%), with the largest fraction (EMPRESA DE PESQUISA ENERGÉTICA, 2020). Figure 1 ahead shows the percentage of different sources on the primary energy production ranging from 2010 to 2019. One can easily see the still massive presence of petroleum on total primary energy production, and the constant presence of sugar cane and its products, as presented above.

Figure 1. Fraction of different sources on the total primary energy production.

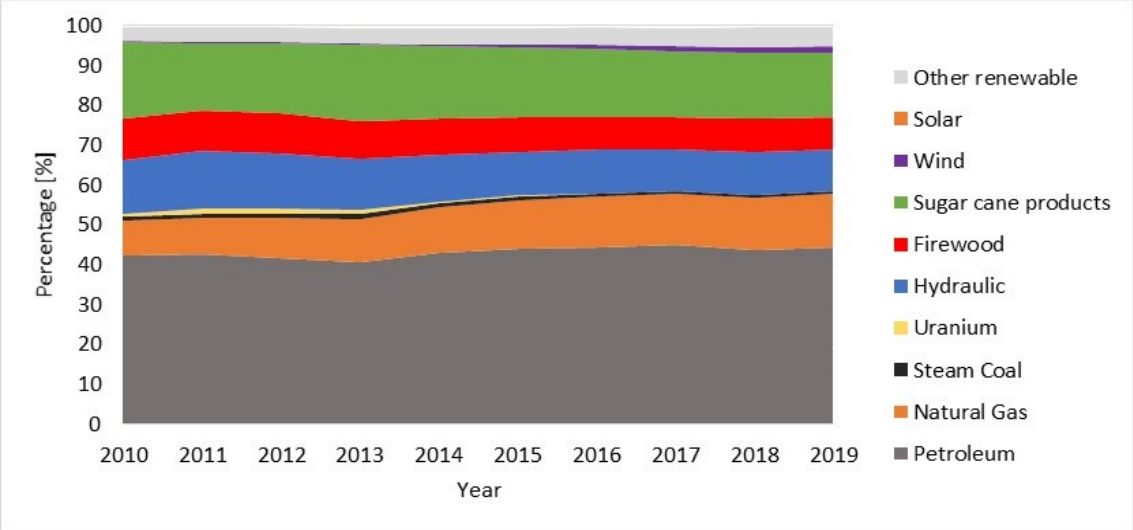

Source: Empresa de Pesquisa Energética (2020), adapted by the author.

Nevertheless, sugar cane has a seasonal harvest, commonly from April to November in the southwest of Brazil, region with the highest share of sugar cane plantations, meaning that outside this period, the cogeneration power plants are not operational, hence, no electricity is being generated (BURIN et al., 2016). Therefore, the possibility to flexibilize the cogeneration is to generate steam during the operational season from other sources, such as "Concentrated Solar Thermal" (CST), also called "Concentrated Solar Power" (CSP), extending the operational season, is sought.

CST technologies collect the Direct Normal Irradiation (DNI) through mirrors or lenses, concentrating it onto a receiver, transforming it into useful energy as heat, electricity or fuels through different systems, with four most common technologies: parabolic trough, linear Fresnel, solar tower, and parabolic dish (LOVEGROVE; CSIRO, 2012; BLANCO; MILLER; 2017). The first commercial CST plant, composed by parabolic troughs, was

constructed on the USA, in the Mojave Desert on the period of 1981-1991, during the oil crisis, attached to energy policies that supported this initiative (ISLAM et al., 2018). In 2019, the total CST installed capacity was estimated to be 5.5 GW (around 70% of it on Spain and USA), with 2.5 GW under construction, and 1.5 GW under development (SARK; CORONA, 2020). CST costs are still high, but a key feature of technologies such as solar tower is that they can easily be integrated with conventional power plants such as coal or biomass, through hybridization, as well as implement thermal energy storage to increase the power plant flexibility, therefore generating electricity on periods without sun, hence increasing the competitiveness (JIN; HONG, 2012).

Brazil is a continental country, with great DNI levels, the main resource regarding the CST technology, with a large portion of its territory with DNI values more than 2,000 kWh/m².year (VIANA et al., 2010), fitted for CST implementations (SARK; CORONA, 2020). Considering a technical background, several studies were carried approaching CST applications in Brazil. Fichter et al. (2017) analyzed how a CST biomass hybrid power plant in Northeast Brazil could positively contribute to the regularization of energy imbalance on the region and be cost-effective from 2040. Souza and Cavalcante (2017) discuss energy policies regarding CST technologies, focusing on Brazil and China. Their approach shows that, as presented above, a liability to insert CST on both countries is the high levelized cost of electricity (LCOE) associated with the technology, not yet competitive. Burin et al. (2016) studied the integration of CSP linear Fresnel and a sugarcane bagasse cogeneration plant in Campo Grande (Brazil), and their results have shown that this combination can be the key to making CSP economically feasible in Brazil.

Even though several studies exist to provide a background for the technology, due to the high capital costs, added to the lack of local industry, CST projects are most likely still unfeasible in Brazil (SORIA et al., 2015), with no projects yet developed.

Nevertheless, CST is a promising way to generate heat and power for agro-industrial processes in regions with a high solar resource (i.e. > 2,000 kWh/m².y) as in the case of Southwest region (MAAG; OLIVEIRA; OLIVEIRA, 2015). Biomass and CST offer the highest potential for cost reduction together with operation improvement, also with installation potential in regions with lower DNI, but requiring sufficient resources for both parts (LANGER, 2016), but even though sugar cane offers this high potential, studies regarding this thematic are still incipient, especially in Brazil.

Consequently, the main goal of this work is to analyze the sugar cane bagasse spare in a plant located in the city of Pirassununga, SP, Brazil, through a solar central receiver technology for direct steam generation (DSG).

2 METHODS

The work's proposal is to extend the harvest by including CST to produce steam, hence, spare bagasse. This concept is shown in Figure 2 ahead.

Figure 2. Extended harvest season due to CST solar fraction.

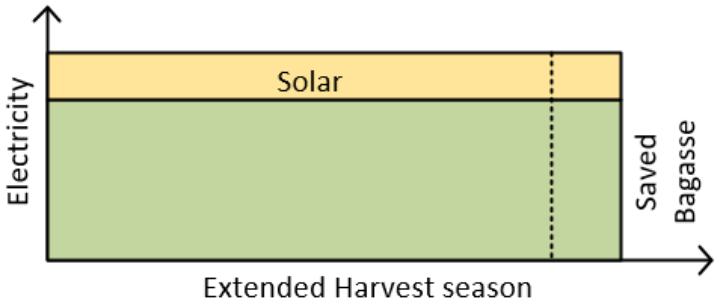

Source: The author.

2.1 Sugar cane power plant

The sugar cane power plant is in Pirassununga (22°00' S, 47°26' W), SP, next to the University of São Paulo (USP) campus where the meteorological data were collected. Raw data were reduced and used in the field layout software *SolarPILOT*, as well as in the numerical simulation on *MATLAB*. *SolarPILOT* stands for "Solar Power Tower Integrated Layout and Optimization Tool" and was developed by the USA National Renewable Energy Laboratory (NREL), through where the user can create heliostat field layouts, constrain positions, model different optical configurations, all of that considering the receiver and atmospheric conditions, and optimize the field layout. *MATLAB* is a programming and numeric computing platform for numerous uses, such as numerical simulation.

In this work, the solar tower is designed to heat water from 45 °C and 65 bar (point 1 in Figure 3) to saturated steam at 280 °C (point 2) before the biomass-superheating boiler. Two turbines of 31.6 MWel and 15.6 MWel, work with 71.2 kg/s live steam at 500 °C and 65 bar (point 3) afterwards, exiting at 150 °C for process (point 4).

Figure 3. Simplified process flow diagram of CST integration.

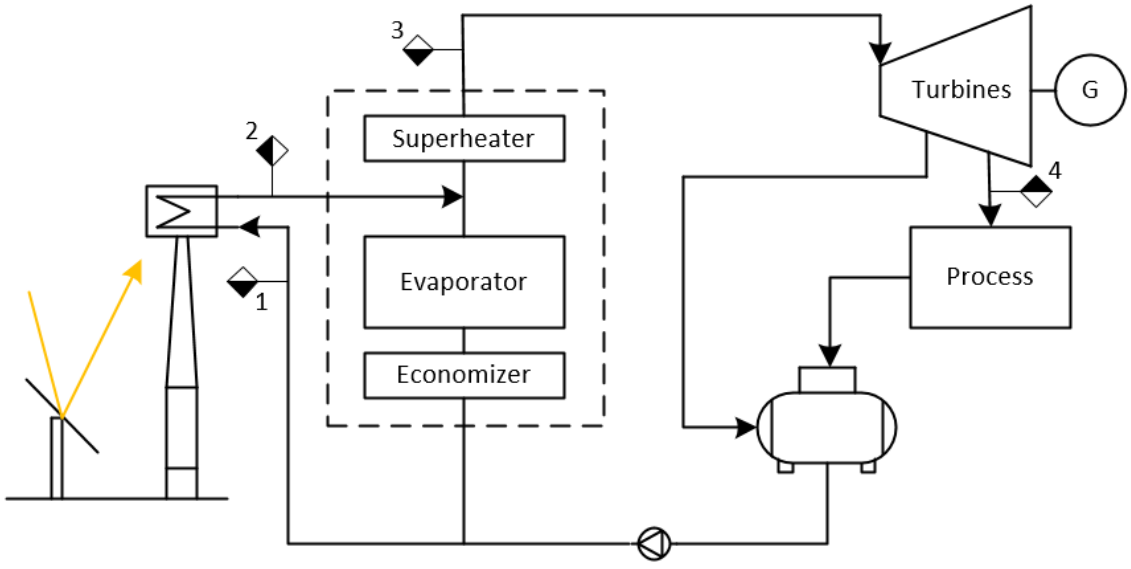

Source: The author.

The available land for the solar field was assessed by Google Earth. Figure 4 shows the solar field, represented in red, with the tower position pinned in yellow, the power plant boiler in green, the bagasse stock in orange, and the

power block in blue. The tower distance to the boiler is approximately 150 m.

Figure 4. Solar field, tower, power block, bagasse stock, and boiler locations within the sugar cane power plant.

Source: The author, with Google Earth.

2.2 SolarPILOT field layout

The ground boundaries (1.12 ha) were applied in the software *SolarPILOT* to determine a solar field layout to directly generate steam in an external cylindrical receiver. No cost assessment was made. The parameters were optimized (e.g. tower optical height, receiver height and diameter, etc.) to increase the overall system efficiency. An adapted rim heliostat like the proposal by Pfahl et al. (2013), with optical height of 2.3 m, was used. The main parameters used in the simulation for the solar field layout generation are summarized in Table 1. Also, the Hermite model with Sigma aiming was applied to determine the receiver flux profile on the summer solstice (21st March) at solar noon.

Table 1. System parameters for solar field layout after optimization.

System parameter	Value
Sunshape model	Gaussian sun
Sunshape angular extend	4.65 mrad
# days/hours simulated	4 days/2 hours frequency
Solar field design power	5.5 MW_{th}
DNI_{design}	850 W/m²
Tower optical height	35 m
Layout method	Radial stagger
Radial spacing method	Eliminate blocking
Heliostat size	9 m² (3x3 m² facets)
Heliostat canting method/focusing type	On-axis at slant/at slant
Mirror reflectivity	0.92
Total reflected image error	2.95 mrad
Receiver height	1.30 m
Receiver diameter	1.70 m
Allowable peak flux	800 kW/m²
Receiver absorptance	0.95

Source: The author.

2.3 Numerical Simulation

The bagasse mass flow in the boiler is 22.45 kg/s, with a 24/7 energy generation in the harvest season, and a bagasse/steam ratio of 0.32. The considered Low Heat Value (LHV) for the bagasse, at 50% humidity, was 7,524 kJ/kg, and boiler efficiency is 0.75 (regarding the LHV) (CENTRO DE TECNOLOGIA CANAVIEIRA, 2010).

Based on the available data set, three arbitrarily days within the harvest were chosen to simulate the spare of bagasse: April 16th, July 16th, and October 16th, 2017, given the transient behavior of DNI on those specific days, as well as monthly analysis throughout the harvest, added to the amount of work which could be generated with the saved biomass were also assessed. The net heat absorbed by the receiver i.e., heat transferred to water, is presented in Eq. (1), whereas Eq. (2) and (3) shows reflection and re-radiation losses (WAGNER, 2008). Pressure losses, as well as conduction losses were neglected.

$$\dot{Q}_{receiver,net} = \dot{Q}_{field} - \left(\dot{Q}_{ref} + \dot{Q}_{rad} + \dot{Q}_{conv}\right) \quad (1)$$

with

$$\dot{Q}_{ref} = \alpha * (T_{receiver} - T_{\infty}) * \dot{Q}_{field} \quad (2)$$

$$\dot{Q}_{rad} = \varepsilon * \sigma * (T^4_{receiver} - T^4_{\infty}) * A_{receiver,abs} \quad (3)$$

Where T_∞ is the ambient temperature; with an assumed solar absorptance α of 0.95 and long wavelengths emittance ε of 0.85 (HO et al., 2012); and σ = 5.6704·10^{-8} W/m^2·K^4 being the Stefan-Boltzmann constant. Natural convection losses were modeled using a vertical flat-plate correlation, as presented by Siebers and Kraabel (1984). All thermophysical properties of the air were calculated based on the film temperature.

$$Nu_{natural} = 0.098.Gr^{\frac{1}{3}}.\left(\frac{T_{receiver}}{T_{\infty}}\right)^{-0.14} \quad (4)$$

$$\bar{h} = \frac{Nu_{natural}.k_{air}}{D_{receiver}} \quad (5)$$

$$\dot{Q}_{conv} = \bar{h} * (T_{receiver} - T_{\infty}) * A_{receiver,abs} \quad (6)$$

The bagasse mass flow to be saved due to CST is represented in Eq. (7). The steam outlet temperature can be controlled through the water mass flow, as in Eq. (8). The receiver is assumed to be at operational temperature ($T_{out,steam}$ + 20 °C) if DNI ≥ 100 W/m², with uniform temperature justified by its small Biot number (0.001) for an assumed 21.3 mm (DN 15) outer pipe diameter with insulation at the back of the tube, and an infinitely quick heat transfer through the tube. No heat transfer and fluid dynamic effects within the tube are considered.

$$\dot{m}_{bagasse} = \frac{\dot{Q}_{receiver,net}}{LHV_{bagasse} * \eta_b} \quad (7)$$

$$\dot{Q}_{receiver,net} = \dot{m}_{water} * \int_{T_{in}}^{T_{out}} c_{p,water}(T_{water}) * dT_{water} \quad (8)$$

3 RESULTS AND DISCUSSION

After optimization, a surrounding solar field layout with 458 heliostats (4,122 m² of mirror area) and average overall design-point field efficiency of 70.9% was found in *SolarPILOT* (Figure 5).

Figure 5. Solar field layout generated with *SolarPILOT*.

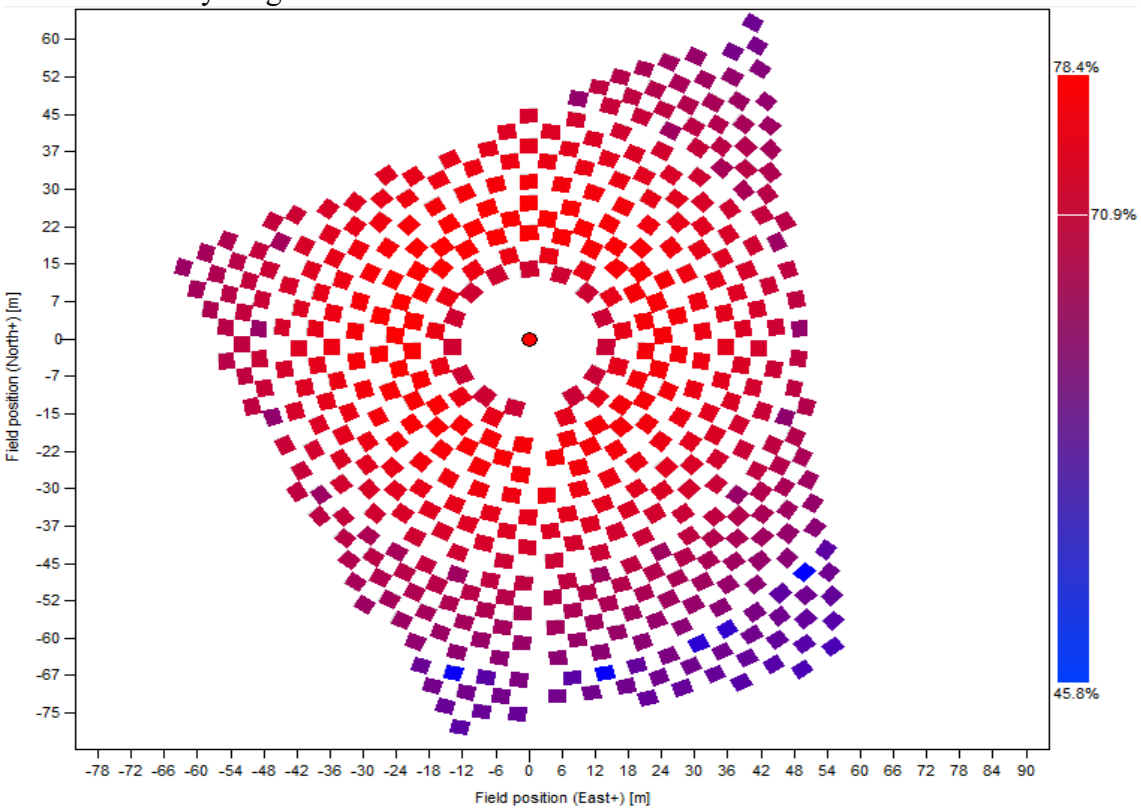

Source: The author.

Table 2 comprises the other solar field efficiencies, whereas Figure 6 shows the external cylindrical solar receiver flux profile obtained on *SolarPILOT*. The peak flux reached was 822.6 kW/m² on the red zones on the receiver's front and back views, whereas the average flux was 327.7 kW/m² for the purple zones.

The solar radiation over the day is dynamic, hence, the receiver has different heating profiles, and the solar flux is incident only half of the tube, creating temperature differentials. In this case the heat flux is slightly above the allowable pear flux, which could overheat the tubes. As presented by Plotkin et al. (2016), forced circulation instead of natural circulation could reduce the risk of overheating, preventing damage.

Table 2. Average design-point solar field efficiencies.

Parameter	Efficiency
Cosine efficiency	89.8%
Blocking efficiency	99.4%
Attenuation efficiency	98.7%
Interception efficiency	91.8%
Soiling Efficiency	95%

Source: The author.

Figure 6. Cylindrical receiver flux profile obtained through analytical simulation.

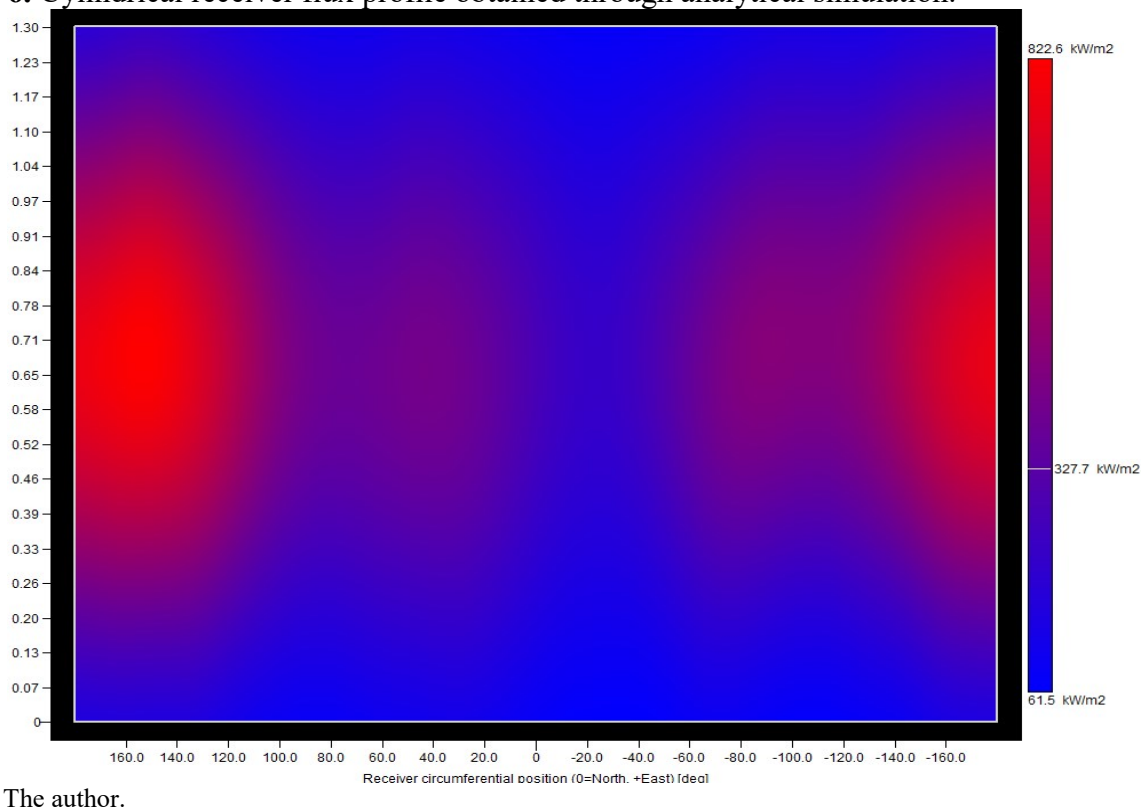

Source: The author.

Figure 7 shows the DNI behavior, the bagasse spared and steam generation for April 16th. As can be seen, the biomass saved and steam generation is proportional to the DNI, declining pari passu with intermittences, as around 15:00, with a significant DNI decrease hence bagasse spare and steam generation.

Figure 7. Bagasse spared, steam generation, DNI for April 16th.

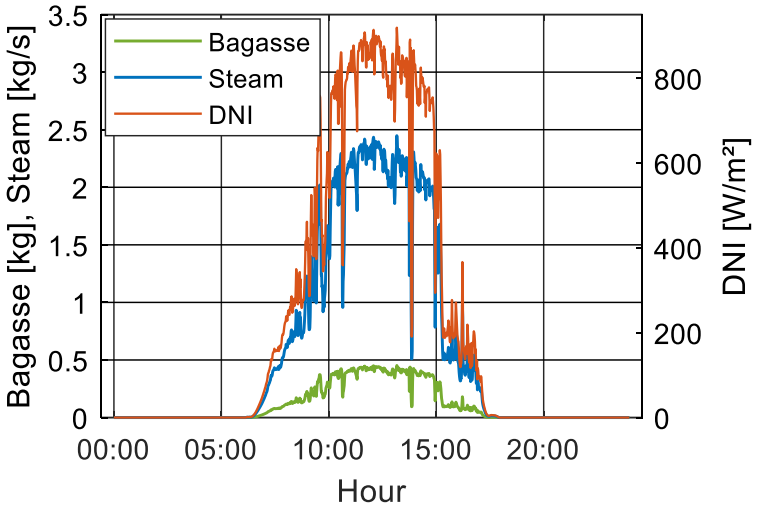

Source: The author.

Figure 8 shows the bagasse spared, steam generation, and DNI for July 16th. Again, as expected, as the DNI decreases, so does the bagasse spare and steam generation, as between 10:00 and 15:00.

Figure 8. Bagasse spared, steam generation, DNI for July 16th.

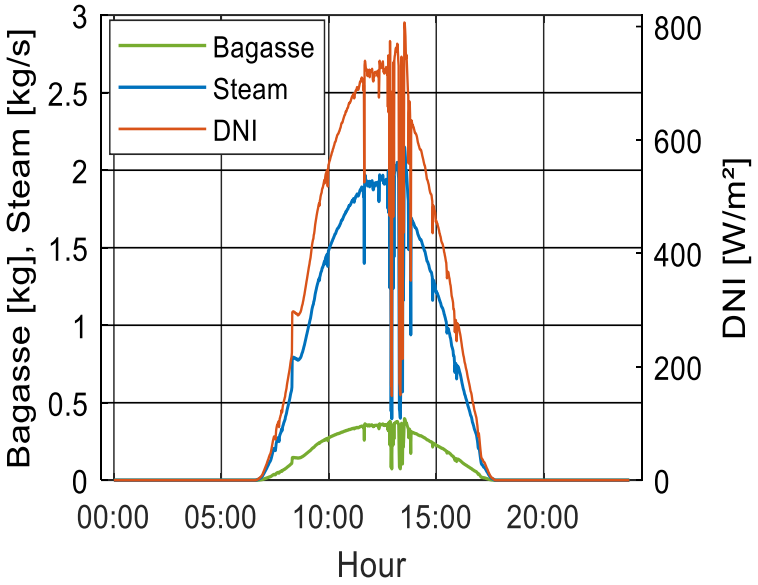

Source: The author.

Figure 9 shows the parameter bagasse spared, steam generation, and DNI for the last day analyzed, October 16th. As depicted in the figures above, when the DNI decreases due to intermittences e.g. clouds, the bagasse spared and steam generation decrease *pari passu*, confirming the proportionality between the first parameter and the last ones.

Figure 9. Bagasse spared, steam generation, DNI for October 16th.

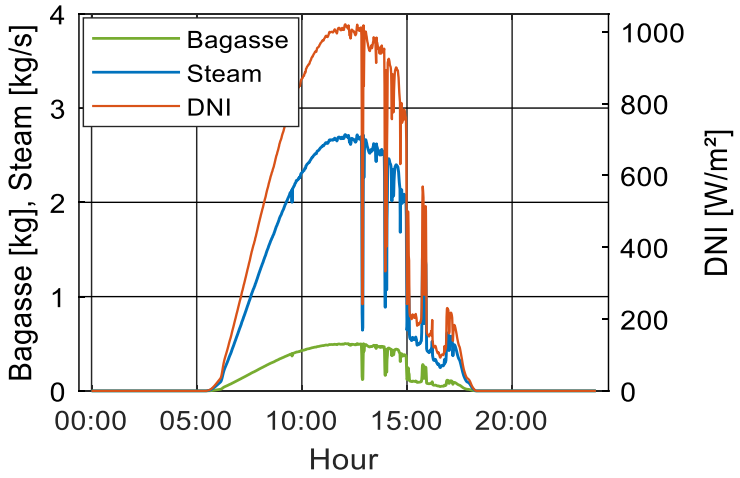

Source: The author.

As a comparison, April 16th presents a more variable incident radiation, behavior also present on July 16th just after noon, and October 16th in the afternoon, reflecting in the bagasse spare and steam generation.

In the best-case scenario, October 16th, the bagasse reached 0.64% of the daily biomass demand, whereas the steam generation was 1.09% of the steam demand. For the less sunny day, July 16th, however, the spare was 0.42%, with steam generation of 0.71% of the daily request, whereas April 16th had an intermediary result, with 0.49% for the biomass, and 0.84% of the steam requirement. These outcomes of daily percentage, as well as the total amount are summarized in Table 3.

Table 3. Total bagasse spared and percentage of total demand for April 16th, July 16th, and October 16th, 2017.

	April 16th	**July 16th**	**October 16th**
Bagasse spared [kg]	9,495.80	8,051.30	12,436.76
% of daily demand	0.49%	0.42%	0.64%
Steam generated [kg]	51,399.46	43,580.59	67,318.46
% of daily demand	0.84%	0.71%	1.09%

Source: The author.

The harvest analysis resulted in 2,127.58 tons of biomass spared, which represent 0.45% of the total amount demanded for a 24/7 electricity generation. Figure 10 shows the monthly energy in MWh in the left y-axis for the solar field, receiver, thermal losses, and solar energy electricity generation; and steam generation and bagasse spared on the right y-axis, all ranging from April to November. The last were the month with the highest insulation, hence, energy and bagasse spared, resulting in 327.4 tons, or 0.56% of the total requirement. In contrast, in June, the bagasse saved was 212.6 tons, corresponding to 0.37% of the total demand. Also, seasonality influence over the energy generation can be observed in Figure 10, decreased over the winter (21st June to 22nd September), and rising again afterward on the spring, from September to the end of the harvest in November.

Figure 10. Monthly incident radiation, net-absorbed heat, losses, and bagasse spared from April to November 2017.

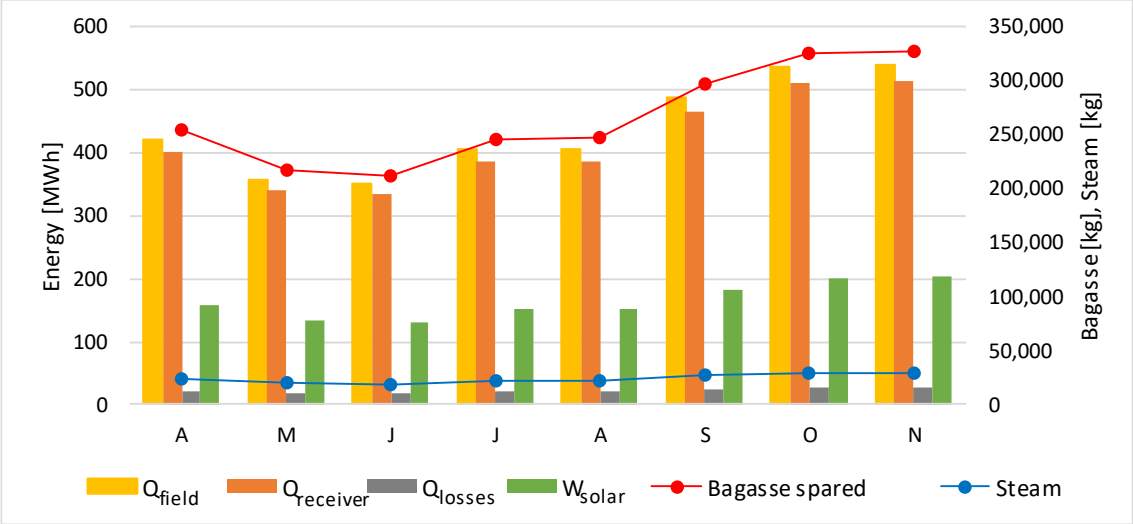

Source: The author.

The total steam generation throughout the harvest was 191,9 tons. Again, November was best case scenario, with 29.5 tons, which represents 0.016% of the monthly demand, whereas June was also the worst-case scenario, resulting in 19.1 tons of steam generation, representing only 0.01% of the monthly requirement. Considering a fix solar field efficiency, the net heat transferred to the water for steam generation i.e., the receiver efficiency resulted in 95.06%.

By applying a power block efficiency of 39.5% (HIRSCH; KHENISSI, 2013), the monthly energy generation by using the spared biomass was calculated, also shown in Figure 10, resulting in 1,317.32 MWh. Considering the ground constraints in the power block surroundings, hence the small scale of the CST plant (field layout for 5.5 MWth), the spared bagasse could fulfill the power plant biomass requirements for electricity generation for 26 more hours only.

3 CONCLUSIONS

A central receiver solar field layout was designed with *SolarPILOT* to partially fulfill the steam requirements of a sugar cane power plant in Pirassununga, São Paulo, Brazil. A numerical simulation with *MATLAB* to predict the spared bagasse was performed for three arbitrary days within the harvest (April 16th, July 16th, and October 16th, 2017), as well as for all harvest, from April to November. The *SolarPILOT* layout resulted in a surrounding field with 458 9 m² heliostats and average design-point efficiency of 0.709. The simulation results show that, for the best-case scenario, October 16th, the CST could spare 12.4 tons of biomass, which represent 0.64% of the daily demand, generating 67.3 tons of steam, or 1.09% of the daily. The monthly analysis shows November as the best-case scenario, with 327.4 tons of bagasse saved, or 0.56% of the total requirement, and 29.5 tons of steam generated, equal to 0.016% of the total demand. For the monthly analysis is possible to observe a seasonality influence over the energy generation, with a decrease over the winter, rising afterwards on spring.

Further studies should approach CST applied on a bigger scale i.e., larger area, considering another power plant, which could increase the bagasse spare in the year. Also, a financial-economical approach could also be performed to assess the feasibility the project though not only a technical but also monetary approach.

4 REFERENCES

BLANCO, M.; MILLER, S. Introduction to concentrating solar thermal (CST) technologies. **Advances In Concentrating Solar Thermal Research and Technology**, [*S. l.*], v. 1, n. 1, p. 3-25, 2017. DOI: http://dx.doi.org/10.1016/b978-0-08-100516-3.00001-0. Available at: https://www.sciencedirect.com/science/article/pii/B9780081005163000010. Accessed on: 6 jun. 2021.

BURIN, E. K.; VOGEL, T.; MULTHAUPT, S.; THELEN, A.; OELJEKLAUS, G.; GÖRNER, K.; BAZZO, E. Thermodynamic and economic evaluation of a solar aided sugarcane bagasse cogeneration power plant. **Energy**, [*S. l.*], v. 117, n. 2, p. 416-428, dec. 2016. DOI: http://dx.doi.org/10.1016/j.energy.2016.06.071. Available at: https://www.sciencedirect.com/science/article/pii/S0360544216308453. Accessed on: 6 jun. 2021.

CENTRO DE TECNOLOGIA CANAVIEIRA. **Determinação da eficiência elétrica das usinas brasileiras para produção exclusiva de açúcar e/ou etanol**. Piracicaba: CTC, 2010. Available at: https://pt.scribd.com/document/62680415/CTC-avalia-eficiencia-do-setor-na-geracao-de-energia-eletrica. Accessed on: 13 mar. 2019.

EMPRESA DE PESQUISA ENERGÉTICA. **Balanço Energético Nacional 2018**: Ano Base 2017. Rio de Janeiro: EPE, 2018.

EMPRESA DE PESQUISA ENERGÉTICA. **Balanço Energético Nacional 2020**: Ano Base 2019. Rio de Janeiro: EPE, 2020.

FICHTER, T.; SORIA, R.; SZKLO, A.; SCHAEFFER, R.; LUCENA, A. Assessing the potential role of concentrated solar power (CSP) for the northeast power system of Brazil using a detailed power system model. **Energy**, [*S. l.*], v. 121, n. 1, p. 695-715, fev. 2017. DOI: http://dx.doi.org/10.1016/j.energy.2017.01.012. Available at: https://www.sciencedirect.com/science/article/pii/S0360544217300129. Accessed on: 6 jun. 2021.

HIRSCH, T.; KHENISSI, A. A Systematic Comparison on Power Block Efficiencies for CSP Plants with Direct Steam Generation. **Energy Procedia**, Amsterdam, v. 49, n. 1, p. 1165-1176, 2014. DOI: http://dx.doi.org/10.1016/j.egypro.2014.03.126. Available at: https://www.sciencedirect.com/science/article/pii/S1876610214005803. Accessed on: 6 jun. 2021.

HO, C.; MAHONEY, A. R.; AMBROSINI, A.; BENCOMO, M.; HALL, A.; LAMBERT, T. Characterization of Pyromark 2500 for High-Temperature Solar Receivers. *In*: INTERNATIONAL CONFERENCE ON ENERGY SUSTAINABILITY, 6.; INTERNATIONAL CONFERENCE ON FUEL CELL SCIENCE, ENGINEERING AND TECHNOLOGY, 10., 2012, San Diego. **Proceedings** […]. San Diego: ASMA, 2012. DOI: https://doi.org/10.1115/ES2012-91374. Available at: https://asmedigitalcollection.asme.org/ES/proceedings-abstract/ES2012/44816/509/232106. Accessed on: 6 jun. 2021.

ISLAM, T.; HUDA, N.; ABDULLAH, A. B.; SAIDUR, R. A comprehensive review of state-of-the-art concentrating solar power (CSP) technologies: Current status and research trends. **Renewable and Sustainable Energy Reviews**, Oxford, v. 91, n. 1, p. 987-1018, ago. 2018. DOI:

http://dx.doi.org/10.1016/j.rser.2018.04.097. Available at: https://www.sciencedirect.com/science/article/pii/S1364032118303113. Accessed on: 6 jun. 2021.

JIN, H. G.; HONG, H. Hybridization of concentrating solar power (CSP) with fossil fuel power plants. **Concentrating Solar Power Technology**, [*S. l.*], v. 1, n. 1, p. 395-420, 2012. DOI: http://dx.doi.org/10.1533/9780857096173.2.395. Available at: https://www.sciencedirect.com/science/article/pii/B9781845697693500121. Accessed on: 6 jun. 2021.

LANGER, N. **Survey of Potential Hybridisation Options for Concentrating Solar Power Plants in Brazil**. 2016. Thesis (Bachelor in Industrial Engineering) – University of Duisburg-Essen, Duisburg, 2016.

LOVEGROVE, K.; CSIRO, W. S. Introduction to concentrating solar power (CSP) technology. **Concentrating Solar Power Technology**, [*S. l.*], v. 1, n. 1, p. 3-15, 2012. DOI: http://dx.doi.org/10.1533/9780857096173.1.3. Available at: https://www.sciencedirect.com/science/article/pii/B9781845697693500017. Accessed on: 6 jun. 2021.

MAAG, G.; OLIVEIRA, K. T.; OLIVEIRA, C. E. L. Hybrid Solar Tower Pilot Plants for Co-Generation of Heat and Power for Brazilian Agro-Industry. *In*: ISES SOLAR WORLD CONGRESS, 2015, Daegu. **Proceedings** […]. Daegu: International Solar Energy Society, 2015. DOI: doi:10.18086/swc.2015.04.22. Available at: http://proceedings.ises.org/paper/swc2015/swc2015-0084-Maag.pdf. Accessed on: 6 jun. 2021.

PFAHL, A.; RANDT, M.; HOLZE, C.; UNTERSCHÜTZ, S. Autonomous light-weight heliostat with rim drives. **Solar Energy**, Oxford, v. 92, n. 1, p. 230-240, jun. 2013. DOI: http://dx.doi.org/10.1016/j.solener.2013.03.005. Available at: https://www.sciencedirect.com/science/article/pii/S0038092X13001023. Accessed on: 6 jun. 2021.

PLOTKIN, A.; TOUPIN, K.; GILLUM, C.; RANCATORE, R.; YANG, T.; MIER, D. Solar Receiver Steam Generator Design for the Ivanpah Solar Electric Generating System. *In*: ASME POWER CONFERENCE, 2011, Denver. **Proceedings** […]. Denver: ASME, 2011. DOI: https://doi.org/10.1115/POWER2011-55248. Available at: https://asmedigitalcollection.asme.org/POWER/proceedings-abstract/POWER2011/44601/523/357664. Accessed on: 6 jun. 2021.

RAMOS, R. C.; NACHILUK, K. Geração de Bioenergia de Biomassa da Cana-de-açúcar nas Usinas Signatárias ao Protocolo Agroambiental Paulista, Safra 2015/2016. **Análises e Indicadores do Agronegócio**, São Paulo, v. 12, n. 4, p. 7, apr. 2017. Available at: http://www.iea.sp.gov.br/ftpiea/AIA/AIA-19-2017.pdf. Accessed on: 31 oct. 2018.

SARK, W.; CORONA, B. Concentrating solar power. **Technological Learning in The Transition to a Low-Carbon Energy System**, [*S. l.*], v. 1, n. 1, p. 221-231, 2020. DOI: http://dx.doi.org/10.1016/b978-0-12-818762-3.00012-1. Available at: https://www.sciencedirect.com/science/article/pii/B9780128187623000121. Accessed on: 6 jun. 2021.

SIEBERS, D. L.; KRAABEL, J. S. **Estimating convective energy losses from solar central receivers**. Livermore: Sandia National Laboratory, 1984. DOI: https://doi.org/10.2172/6906848. Available at: https://www.osti.gov/servlets/purl/6906848. Accessed on: 6 jun. 2021.

SORIA, R.; PORTUGAL-PEREIRA, J.; SZKLO, A.; MILANI, R.; SCHAEFFER, R. Hybrid concentrated solar power (CSP)–biomass plants in a semiarid region: a strategy for CSP deployment in Brazil. **Energy Policy**, London, v. 86, n. 1, p. 57-72, nov. 2015. DOI: http://dx.doi.org/10.1016/j.enpol.2015.06.028. Available at: https://www.sciencedirect.com/science/article/pii/S0301421515002463. Accessed on: 6 jun. 2021.

SOUZA, L. E. V.; CAVALCANTE, A. M. G. Concentrated Solar Power deployment in emerging economies: the cases of China and Brazil. **Renewable And Sustainable Energy Reviews**, Oxford, v. 72, n. 1, p. 1094-1103, may 2017. DOI: http://dx.doi.org/10.1016/j.rser.2016.10.027. Available at: https://www.sciencedirect.com/science/article/pii/S136403211630675X. Accessed on: 6 jun. 2021.

VIANA, T. S.; RÜTHER, R.; MARTINS, F. R.; PEREIRA, E. B. Assessing the potential of concentrating solar photovoltaic generation in Brazil with satellite-derived direct normal irradiation. **Solar Energy**, Oxford, v. 85, n. 3, p. 486-495, mar. 2011. DOI: http://dx.doi.org/10.1016/j.solener.2010.12.015. Available at: https://www.sciencedirect.com/science/article/pii/S0038092X10003944. Accessed on: 6 jun. 2021.

WAGNER, M. **Simulation and Predictive Performance Modeling of Utility-Scale Central Receiver System Power Plants**. 2008. Thesis (Doctorate in Mechanical Engineering) – University of Wisconsin-Madison, Madison, 2008.